Title	β decay of ^{38,40}Si (T_z = +5, +6) to low-lying core excited states in odd-odd ^{38,40}P isotopes
Author(s)	Tripathi V., Lubna R. S., Abromeit B., Crawford H. L., Liddick S. N., Utsuno Yutaka, Bender P. C., Crider B. P., Dungan R., Fallon P., Kravvaris K., Larson N., Macchiavelli A. O., Otsuka Takaharu, Prokop C. J., Richard A. L., Shimizu Noritaka, Tabor S. L., Volya A., Yoshida Sota
Citation	Physical Review C, 95(2), p.024308_1-024308_7
Text Version	Publisher's Version
URL	https://jopss.jaea.go.jp/search/servlet/search?5058233
DOI	https://doi.org/10.1103/PhysRevC.95.024308
Right	

β decay of ^{38,40}Si ($T_z = +5, +6$) to low-lying core excited states in odd-odd ^{38,40}P isotopes

Vandana Tripathi,[1] R. S. Lubna,[1] B. Abromeit,[1] H. L. Crawford,[2] S. N. Liddick,[3,4] Y. Utsuno,[5,6] P. C. Bender,[4] B. P. Crider,[4] R. Dungan,[1] P. Fallon,[2] K. Kravvaris,[1] N. Larson,[3,4] A. O. Macchiavelli,[1] T. Otsuka,[7,4,8] C. J. Prokop,[3,4] A. L. Richard,[9] N. Shimizu,[6] S. L. Tabor,[1] A. Volya,[1] and S. Yoshida[7]

[1]*Department of Physics, Florida State University, Tallahassee, Florida 32306, USA*
[2]*Nuclear Science Division, Lawrence Berkeley National Laboratory, Berkeley, California 94720, USA*
[3]*Department of Chemistry, Michigan State University, East Lansing, Michigan 48824, USA*
[4]*National Superconducting Cyclotron Laboratory, Michigan State University, East Lansing, Michigan 48824, USA*
[5]*Advanced Science Research Center, Japan Atomic Energy Agency, Tokai, Ibaraki 319-1195, Japan*
[6]*Center of Nuclear Study, University of Tokyo, Hongo, Bunkyo-ku, Tokyo 113-0033, Japan*
[7]*Department of Physics, University of Tokyo, Hongo, Bunkyo-ku, Tokyo 113-0033, Japan*
[8]*Instituut voor Kern- en Stralingsfysica, Katholieke Universiteit Leuven, B-3001 Leuven, Belgium*
[9]*Institute of Nuclear and Particle Physics, Department of Physics and Astronomy, Ohio University, Athens, Ohio 45701, USA*

(Received 16 November 2016; revised manuscript received 18 January 2017; published 8 February 2017)

Low-lying excited states in ^{38,40}P have been identified in the β decay of $T_z = +5, +6$, ^{38,40}Si. Based on the allowed nature of the Gamow-Teller (GT) decay observed, these states are assigned spin and parity of 1^+ and are core-excited 1p1h intruder states with a parity opposite to the ground state. The occurrence of intruder states at low energies highlights the importance of pairing and quadrupole correlation energies in lowering the intruder states despite the $N = 20$ shell gap. Configuration interaction shell model calculations with the state-of-art SDPF-MU effective interaction were performed to understand the structure of these 1p1h states in the even-A phosphorus isotopes. States in ^{40}P with $N = 25$ were found to have very complex configurations involving all the fp orbitals leading to deformed states as seen in neutron-rich nuclei with $N \approx 28$. The calculated GT matrix elements for the β decay highlight the dominance of the decay of the core neutrons rather than the valence neutrons.

DOI: 10.1103/PhysRevC.95.024308

I. INTRODUCTION

In the quest for a realistic model of nuclei with strong predictive powers, the need remains for far more wide-ranging experimental information on nuclei across the chart of nuclides. As we seek to understand the evolution of shell structure toward the drip lines [1,2] expanded information on excited states is required; intruder states arising from reduced single-particle level spacings and correlations are of particular interest. Though they are the least investigated, odd-Z and/or odd-odd nuclei provide one of the most stringent tests of theoretical predictions because of the additional degrees of freedom available. The details of the proton-neutron interaction and the couplings within the proton and neutron valence spaces play a key role in the excitation spectra of odd-odd nuclei [3].

In this paper we report on the low-lying core-excited states in the neutron-rich odd-odd phosphorus isotopes, namely ^{38,40}P with $N = 23$ and 25, respectively. The ground states of these nuclei have negative parity arising from the coupling of the unpaired fp neutron and sd proton. However, promoting one neutron across the $N = 20$ shell gap allows the fp neutrons to be paired and the resulting hole in the sd shell can couple with the sd proton leading to positive parity states. Such core-excited one-particle–one-hole (1p1h) states contain information about the $N = 20$ and $N = 28$ shell gaps. Tracking the excitation energy of the 1p1h states as a function of neutron number can allow us to infer how the proton-neutron interaction evolves with neutron excess. One of the biggest hurdles in this understanding is the missing information on parities leading to uncertainties in the position of the intruder states. Allowed β decay is one tool that can lead to a definitive range in spin and parity for excited states provided the spin and parity of the parent is known [4]. In this work we used β decay of ^{38,40}Si to populate excited states in the daughter nuclei and the measured $\log ft$ values to reliably constrain their spin and parity. The even-mass Si isotopes have 0^+ as their ground state leading to the population of 1^+ states in allowed β decay. These 1^+ states are 1p1h states having a parity opposite to the ground state. Population of core-excited states should not be favored, in general, due to the reduction in the energy released; however, in neutron-rich nuclei the β decay is likely to proceed via the decay of the core neutrons [5,6].

Prior to this work, no excited states were observed in ^{40}P and a lone tentative 380-keV transition was assigned to ^{38}P corresponding to the depopulation of a low-lying yrast state [7]. Based on the allowed β decay of ^{38,40}Si we have identified 1^+ states in both ^{38,40}P. These states lie at relatively low excitation energies of $\sim$2 MeV. This is in contrast to recent results on the decay of neutron-rich zinc and gallium isotopes near ^{78}Ni [5,6], where Gamow-Teller (GT) β transitions populated high-lying core-excited states in the daughter nuclei. The experimental results are interpreted within configuration interaction shell model calculations using the SDPF-MU interaction [9]. Additionally, the half-life of the parent ^{38}Si has also been measured for the first time, as well as β-delayed neutron emission probabilities (P_n) for ^{38,40}Si.

II. EXPERIMENTAL DETAILS

The experiment to investigate the β decay of ^{38,40}Si was carried out at the National Superconducting Cyclotron

Laboratory (NSCL) [10] at Michigan State University. A 140 MeV/u ^{48}Ca primary beam was fragmented in a Be target of thickness 795 mg/cm^2 at the target position of the fragment separator, A1900 [11], to produce the nuclei of interest. A wedge-shaped Al degrader (45 mg/cm^2) was used at the intermediate dispersive image of A1900 for further energy dispersion. With a full momentum acceptance of 5.08% of the A1900 (rigidities set to 4.705, 4.660, and 4.23 Tm), a cocktail beam centered around ^{36}Mg was obtained at the focal plane. This mix of exotic isotopes was transported to the β counting system where they were implanted in a 1-cm-thick 16 × 16 segmented planar germanium double-sided strip detector (GeDSSD) [12], which recorded the time and position of implants, as well as subsequent decays. The implant rate was kept low, around 100 Hz, so as to maximize the efficiency of correlating the implanted ion with the decay products. The high-energy implants and the low-energy β particles were processed separately with low- and high-gain preamplifiers, respectively. A Si PIN detector placed before the GeDSSD provided the energy loss and time-of-flight information (along with the scintillator at the intermediate dispersive image of the A1900) for particle identification of the incoming implants. The GeDSSD was surrounded by 16 detectors of the segmented germanium array (SeGA) [13] to record the β-delayed γ rays with an efficiency of about 3.5% at 1 MeV.

The data were collected event by event using the NSCL digital data acquisition system [14]. Each channel provided its own time-stamp signal, which allowed coincidences and correlations to be built in the analysis. The high-gain energy signals from the GeDSSD were used to isolate a decay event which was subsequently correlated to an implanted ion (low-gain energy signal) in the same pixel within a fixed time. β-delayed γ rays emitted from excited states of the daughter nuclei were selected by looking for coincidences with β-decay electrons correlated to a specific implanted ion within a specified time window. Each SeGA detector was individually energy calibrated and the calibrated outputs were summed together to generate a delayed γ spectrum for a particular correlation time. γ-γ matrices were also generated to look for coincidences.

III. RESULTS AND DISCUSSION

The time differences between a ^{40}Si implant and the correlated β particles were histogrammed up to 1000 ms after the initial implant to generate the decay curve shown in Fig. 1(a). Taking into consideration the decay of the initial implant, the decay of the daughter and the β-delayed neutron emission daughter, the decay curve was fitted using the Bateman equation along with an exponential background [15].

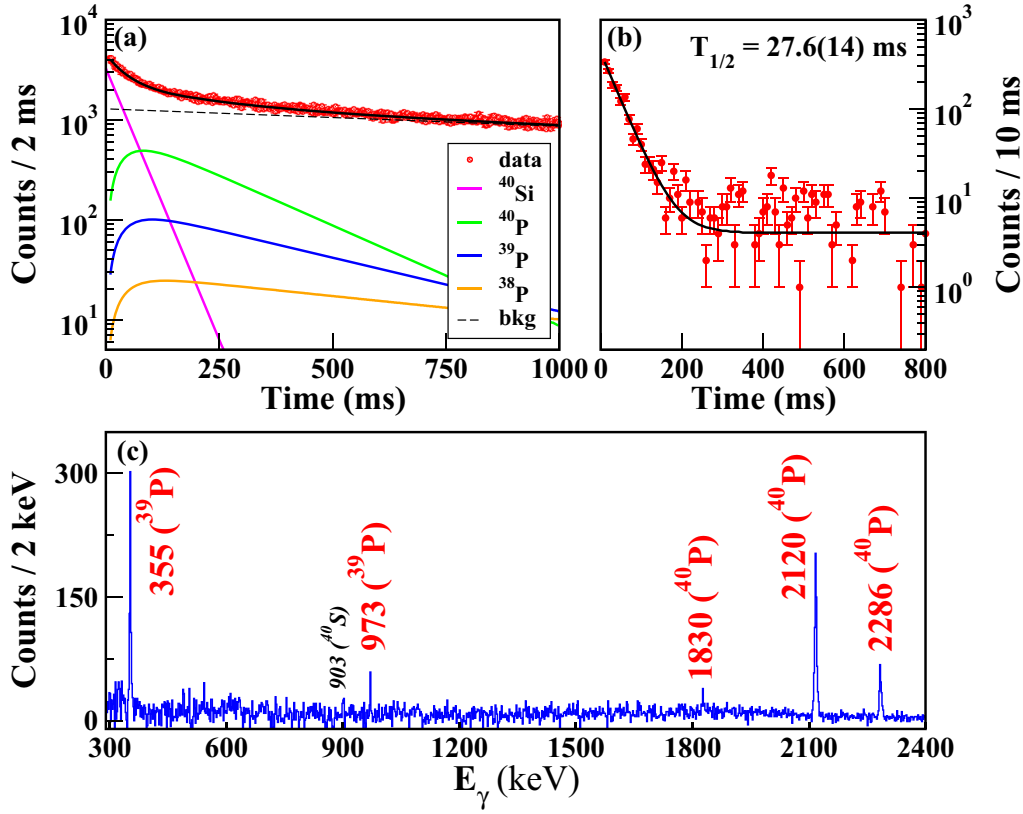

FIG. 1. (a) Decay curve derived for ^{40}Si from β-correlated implants within the same pixel for 1000 ms along with the fit used to extract half-life and the initial activity. The components of the fit are (i) exponential decay of parent, ^{40}Si, (ii) exponential growth and decay of daughter nuclei, ^{40}P (β), ^{39}P (β-n), ^{38}P ($\beta - 2n$), and (iii) exponential background. Known half-lives were used for the daughter nuclides [18]. (b) Decay curve from (a) in coincidence with γ transitions in the daughter ^{40}P. The data are fitted to an exponential decay function with a constant background. (c) Partial β-delayed γ spectrum observed for 30 ms after a ^{40}Si implant, with the new transitions in ^{40}P marked by energy, as well as those from ^{39}P populated in β-delayed one-neutron emission.

TABLE I. Experimental (present and previous) and shell model (SM) estimates of the half-life ($T_{1/2}$) and β-delayed neutron emission probability (P_n) for ^{36,38,40}Si. Literature values are from Refs. [8,16]. For the shell model calculations experimental masses were used and the uncertainties in the calculated half-lives and neutron emission probabilities arise from the uncertainties in the experimental masses [17].

Isotope	$T_{1/2}$(ms)			P_n(%)		
	Present	Previous	SM	Present	Previous	SM
^{36}Si		450(60)	310(20)		<10	3.7(4)
^{38}Si	63(8)	(>1 μs)	77(5)	25(10)		20(1)
^{40}Si	27.6(14)	33.0(10)	26(4)	38(5)		28(1)

The multiparameter fit gave a half-life of 27(1) ms for ^{40}Si, somewhat shorter than the previously measured value of 33.0(10) ms [8]. The biggest uncertainty in this fit is the background which arises from the decay of all implanted nuclei and their longer lived daughter activities. To overcome this uncertainty, the decay curve in coincidence with the two strongest γ transitions in ^{40}P (discussed next) is shown in Fig. 1(b). A fit using a simple exponential function with two parameters and a constant background gave a half-life of 27.6(14) ms. The presented value in the current work agrees well with the shell model estimates using the SDPF-MU interaction discussed later (see Table I).

The β-delayed γ spectrum following a β-correlated ^{40}Si implant in a 30-ms time window is shown in Fig. 1(c), from which a random correlation γ spectrum has been subtracted. The random correlation γ spectrum was generated for times longer than 500 ms after the implant and was able to eliminate the long-lived daughter activities of ^{40}Si decay, as well as those of the more intense implants. Of the transitions seen in Fig. 1(c), the 355- and 973-keV are known to belong to ^{39}P [19], the β-n daughter. The new γ transitions at 2120(1) and 2286(1) keV do not show any coincidences with either of the decays in ^{39}P. Further they are too intense to be ground-state decays in ^{39}P because that would lead to unrealistically large delayed neutron emission probability (see Table I for shell model predictions). Thus the two most intense new transitions at 2120(1) and 2286(1) keV and the weak 1830(1) keV are proposed to be the first γ transitions observed in ^{40}P, with relative intensities of 100%, 31(2)%, and 7(1)%, respectively. The decay curve gated by the 2120- and 2286-keV transitions was discussed previously [Fig. 1(b)]. The weak 903-keV transition is from the daughter activity ($2^+ \rightarrow 0^+$ in ^{40}S) [18]. No γ-γ coincidences were observed; hence, the three transitions are assumed to populate directly the ground state of ^{40}P.

A similar analysis was done for the ^{38}Si implants. However, the statistics here were very limited due to the settings of the A1900 for this experiment. The decay curve for ^{38}Si is shown in Fig. 2. A multiparameter fit including daughter and β-n daughter decay yields a half-life of 63(8) ms, in good agreement with the shell model calculations (Table I). The β-delayed γ spectrum collected for 50 ms after the ^{38}Si implant (inset of Fig. 2) shows two γ transitions at 1874(1) keV (100%)

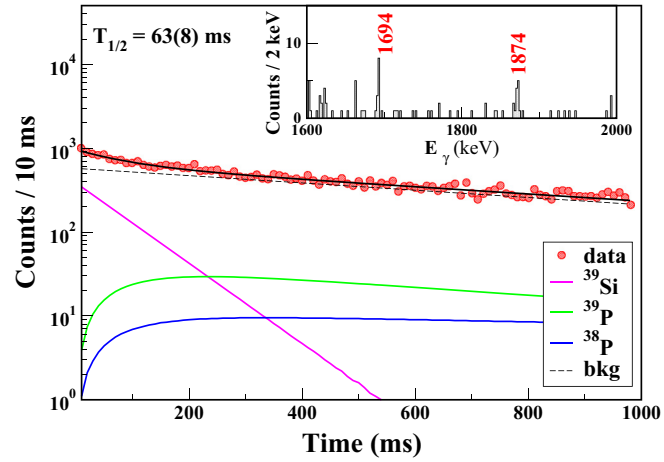

FIG. 2. Time difference between a ^{38}Si implant and an electron detected within the same pixel. A multiparameter fit to the decay curve following the Bateman equations gave the first measure of the half-life of ^{38}Si at 63(8) ms. The inset shows the β-delayed γ spectrum observed for 50 ms after a ^{38}Si implant, showing the new transitions in the daughter nucleus ^{38}P.

and 1694(1) keV [34(9)%] which have been associated with the daughter nucleus, ^{38}P. A third weak transition at 1120(2) is also tentatively assigned to ^{38}P. All three are assumed to be transitions to the ground state similar to ^{40}P. γ transitions in ^{37}P [20] arising from β-delayed neutron emission are also seen at 861 and 1300 keV.

The partial level schemes of ^{38,40}P, as established in the present β-decay study are shown in Fig. 3. In each nucleus two states are dominantly populated with the weak population of a third state. The net direct feeding to these states was normalized to the total correlated implants produced to obtain the absolute β-decay branching per 100 decays. The absolute branching, measured half-life, and Q_{β^-} [17] were used to calculate the logft values [21]. The calculated logft values are consistent with those for allowed β decay, i.e., between

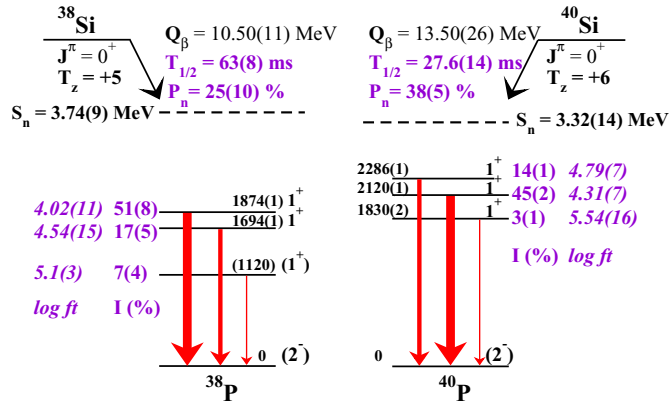

FIG. 3. Partial level schemes of ^{38,40}P as established in the present β^- decay of ^{38,40}Si. The measured half-lives and P_n values are also shown. The measured absolute branching, measured half-life, and Q_{β^-} [18] were used to calculate the logft values [21] which fall in the range for allowed GT transitions.

TABLE II. Results of shell-model calculations using the SDPF-MU interaction for the 1^+ state above neutron separation energy (S_n) for ^{38,40}P (excitation energies and corresponding $\log ft$ values for the first 10 unbound 1^+ states).

^{38}P		^{40}P	
E^*(keV)	$\log ft$	E^*(keV)	$\log ft$
3749	5.63	3558	6.61
3968	7.81	3854	6.35
4040	4.38	3992	7.11
4192	5.47	4098	6.56
4244	6.32	4297	4.86
4313	5.47	4347	7.82
4464	5.35	4886	5.12
4521	5.67	4962	4.83
4561	6.61	5081	6.38
4700	5.13	5174	6.02

4 and 6 [4]. As the parent nucleus (even-even) has a ground state J^π of 0^+, the observed excited states in both ^{38,40}P are assigned a J^π of 1^+. For ^{40}Si decay, the bound states in the daughter exhaust 62% of the β-decay strength. The remaining strength is proposed to go to neutron unbound states lying above 3.32(14) MeV, assuming no feeding to the ground state which has negative parity, and therefore is not populated in allowed decay. Up to the neutron threshold for ^{40}P at 3.32(14) MeV, SeGA has significant efficiency for γ detection ($\sim$1% for a 4.5-MeV γ) and thus it is not likely that any strong transitions from bound states are missed. The calculated delayed neutron emission probability P_n is 38(5)%, of which 20% is observed to go to the first two excited states in the β-n daughter, ^{39}P, at 355 ($\frac{3}{2}^+$) and 973 keV ($\frac{5}{2}^+$). Neutron emission leading to the ground state of ^{39}P is also allowed by a $l = 0$ neutron which will not be accompanied by any γ emission. For ^{38}Si decay, the P_n is calculated to be 25(10)% with the larger errors stemming from the poor statistics. The measured P_n values are compared with the shell model estimates in Table I and show good agreement. The calculations predict several 1^+ states above the neutron threshold (Table II) which are likely responsible for the delayed neutron emission.

The ground state of ^{36}P with $N = 21$ has a J^π of 4^- with a 3^- excited state at 250 keV [22]. The ground-state doublet arises from the $[\pi(s_{1/2}) \otimes \nu(f_{7/2})]^{3^-,4^-}$ configuration in a simple shell model picture. With two and four extra neutrons in ^{38}P and ^{40}P, respectively, the ground states are predicted to be 2^- [7]. One possible configuration arises from the $[\pi(d_{3/2}) \otimes \nu(f_{7/2})]^{2^- to 5^-}$ coupling. This implies occupancy of the $\pi d_{3/2}$ orbital instead of $\pi s_{1/2}$, potentially pointing to the reduction of the $s_{1/2}$-$d_{3/2}$ spacing as neutrons are added to the $f_{7/2}$ orbital [23]. Also with the increase in neutron number, the $(f_{7/2})^3$ and $(f_{7/2})^5$ configurations of the valence neutrons in the ^{38,40}P ground state, respectively, start to favor $\frac{5}{2}^-$ over $\frac{7}{2}^-$ (as in ^{36}P), similar to the ground-state configuration of ^{37}Si [24]. This configuration of the valence neutrons favored in the shell model calculations, along with the $s_{1/2}$ proton, $[\frac{1}{2}^+ \otimes \frac{5}{2}^-]^{2^-,3^-}$ can also explain the switching of the ground state from 4^- in ^{36}P to 2^- in ^{38,40}P. The decay of the observed 1^+ states in ^{38,40}P directly and solely to the ground state most likely by fast $E1$ transitions is consistent with the 2^- prediction for the ground state and rules out the 3^- and 4^- possibilities. The direct β^- decay to the 2^- ground state would be a unique first forbidden transition. With a typical $\log ft$ value of 7.5 for such a decay the expected intensity would be 0.05%. This is why we neglected the ground-state branch in calculating the P_n value.

Partial level schemes of odd-odd $^{34-40}$P isotopes are shown in Fig. 4, along with shell model calculations. The level schemes for ^{34,36}P are from the β decay studies of Refs. [22,25]. For ^{34}P ($Z = 15$ and $N = 19$), the lowest configuration is expected to be the $[(\pi s_{1/2})^1(\nu d_{3/2})^{-1}]^{1^+,2^+}$ doublet with 1^+ as the ground state [25]. For the $N > 20$ isotopes, ^{36,38,40}P, the 1^+ states no longer correspond to the lowest energy configuration but rather are excited states formed by promoting a neutron to the fp shell. The β decay from 0^+ states in the corresponding Si isotopes uniquely identifies these 1^+ intruder states. In the β decay of neutron-rich nuclei, with valence protons and neutrons occupying different shells of opposite parity, sd and fp in this case, the decay of the valence neutron can only take place via forbidden transitions to the lowest states in the daughter. However, GT decay of the core neutron is allowed and results in core-excited states in the daughter nucleus, the 1p1h 1^+ states as seen in the present case. These decays should in general be hampered by the phase space as the 1p1h states are expected at high energy. Though for neutron-rich odd-odd phosphorus isotopes we see that the 1p1h states lie at a relatively low energy of around 2 MeV. The phosphorus isotopes lie outside the island of inversion, thus the low excitation energy of the intruder states is due to the gain in pairing energy in the $f_{7/2}$ orbital and the large quadrupole-quadrupole correlation energy involving both neutrons and protons.

The presence of low-lying intruder states with definitive J^π assignments provides an ideal condition to test the *sd-pf* cross shell proton-neutron interaction. Configuration interaction shell-model calculations with the SDPF-MU interaction [9] were performed both for negative-parity 0p0h states and positive-parity 1p1h states in the full *sd-fp* valence space. The single-particle energies (SPEs) and two-body matrix elements (TBMEs) used in the SDPF-MU calculations are based on existing interactions: the USD [26] for the sd shell and GXPF1B [27] for fp shell. The *sd-fp* cross-shell interaction is given by a monopole-based universal interaction, $V_{\rm MU}$ [28]. The $V_{\rm MU}$ includes the tensor force and embodies the shell evolution, i.e., the displacement of single-particle orbitals with neutron excess. To compare theoretical B(GT) values to experimental values, a quenching factor of $q = 0.77$ was used in the SDPF-MU calculations.

For ^{34}P ($N = 19$), three low-lying 1^+ states are predicted including the ground state in good agreement with the experimental data [25] as well as the USD interaction as seen in Fig. 4. The $1^+_{1,2}$ states have the dominant configuration, $[(\pi s_{1/2})^1(\nu d_{3/2})^{-1}]^{1^+}$ and $[(\pi s_{1/2})^1(\nu s_{1/2})^{-1}]^{1^+}$ respectively and are predicted to have a 60% and 40% β-decay branching. In contrast, in the measured β decay of ^{34}Si to ^{34}P [25], 100% of the β-decay strength was assumed to go to the 1^+_2 state

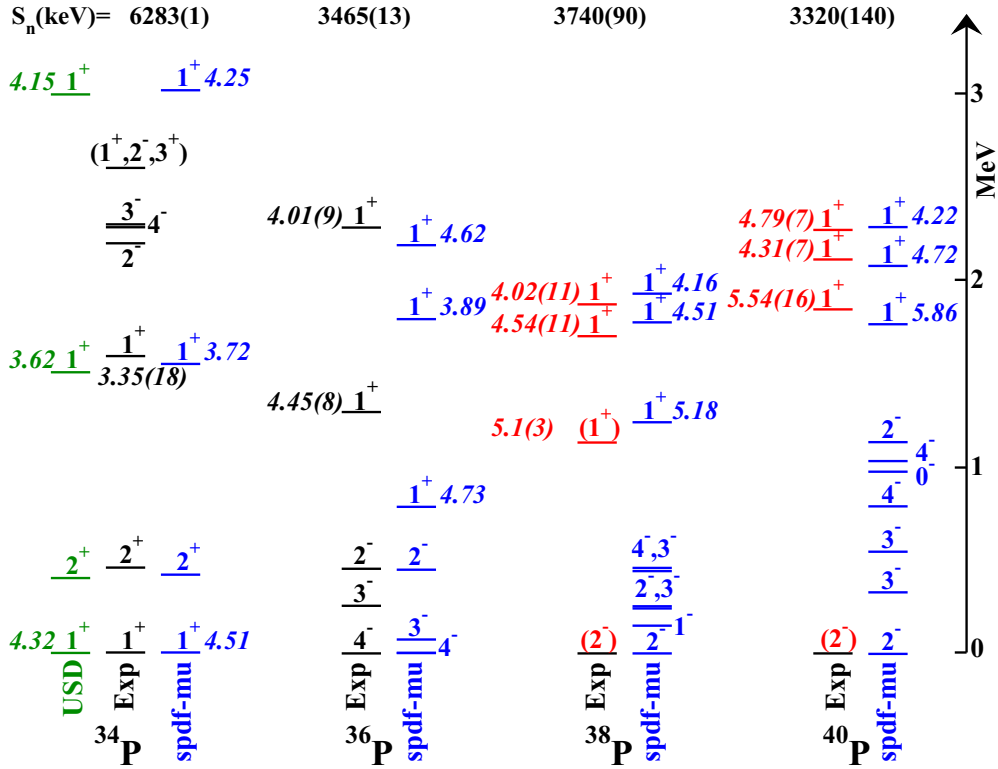

FIG. 4. Partial level schemes of ^{34,36,38,40}P ($N = 19, 21, 23, 25$) as obtained in the β decay of the corresponding Si isotopes. New information from this experiment is depicted in red. Data for ^{34,36}P are from Refs. [22,25]. Results of shell model calculations using the SDPF-MU interaction for all isotopes and calculations based on the USD interaction for ^{34}P are shown. Only calculated bound 1^+ states and few states of other spins relevant to the discussion in this work are displayed. The $\log ft$ values (measured and calculated) for the 1^+ states are marked in italics.

ignoring feeding to the 1^+ ground state. In the case of ^{36}P with $N = 21$, the 1^+ states are 1p1h states with one neutron promoted across the $N = 20$ gap. The SDPF-MU interaction predicts three bound 1^+ states of which the lower two agree quite well with the experimental states for the $\log ft$ values (Fig. 4), but the predicted states are about 500 keV too low in energy (see Table III). For the more neutron-rich isotopes, ^{38,40}P, the calculations again predict three 1^+ states below the neutron separation energy in good agreement with the experimental states, as can be seen in Fig. 4 and Table III. For ^{38}P, the rms deviation is about 83 keV for the three states, whereas for ^{40}P, it is only 39 keV. However, for ^{40}P, a better agreement between the calculated and predicted $\log ft$ values is obtained by swapping the predicted 1^+_2 and 1^+_3 states giving a higher rms deviation of 157 keV, which is still very good for cross-shell states. The better agreement for the 1p1h states in the most neutron-rich isotope ($N = 25$) as compared to ^{36}P suggests that the fp orbitals are pulled down too much for the $N = 21$ isotope in the calculation, similar to the observation in Si isotopes [29].

The calculated proton (sd orbitals) and neutron (sd-fp orbitals) occupancies for the 1^+ states and ground state in odd-odd $^{36-40}$P are shown in Fig. 5. The protons show very little rearrangement for ^{36}P from the simple shell model picture of $(\pi d_{5/2})^6(\pi s_{1/2})^1$. However, for ^{38,40}P there is an increased occupancy of the $\pi d_{3/2}$ orbital as compared to $\pi s_{1/2}$ in the ground-state configuration as well as for the excited states. This is an indication of the near degeneracy of the $\pi s_{1/2}$ and $\pi d_{3/2}$ orbitals as neutrons start filling the $f_{7/2}$ orbital. The valence neutrons meanwhile occupy the fp orbitals. For ^{36}P, they remain predominantly in the $f_{7/2}$ orbital. On the other hand for ^{40}P, the $\nu p_{3/2}$ occupancy increases up to about 1 along with some occupancy of the higher fp orbitals, due

TABLE III. Results of shell model calculations using the SDPF-MU interaction for the 1^+ state (excitation energies and corresponding $\log ft$ values) for odd-odd $^{34-40}$P. The experimentally observed 1^+ states are also shown for comparison.

Isotope	J^π_n	SDPF-MU		Expt.
		E^*(keV)	$\log ft$	E^*(keV)
^{34}P	1^+_1	0	4.51	0
	1^+_2	1523	3.72	1607.77(20)
	1^+_3	3022	4.25	
^{36}P	1^+_1	787	4.73	1303.1(2)
	1^+_2	1809	3.89	2281.0(3)
	1^+_3	2180	4.62	
^{38}P	1^+_1	1231	5.18	1120(2)
	1^+_2	1778	4.51	1694(1)
	1^+_3	1919	4.16	1874(1)
^{40}P	1^+_1	1772	5.86	1830(2)
	1^+_2	2086	4.72	2120(1)
	1^+_3	2296	4.22	2286(1)

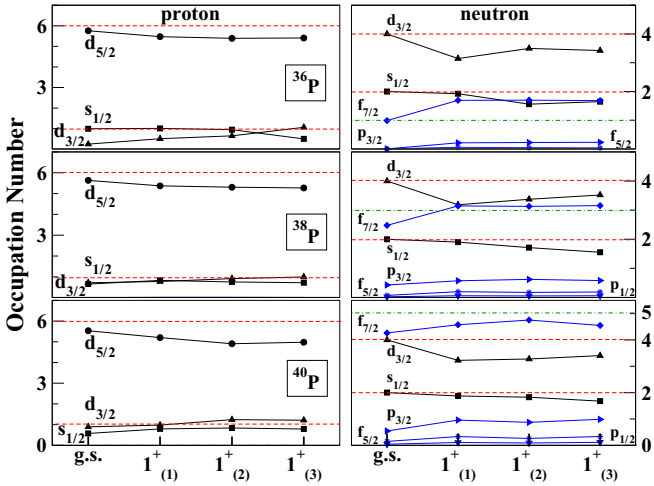

FIG. 5. Calculated proton and neutron occupancies for the ground state and the three excited 1^+ states in ^{36,38,40}P. For protons, the occupancies for the filled orbitals in the extreme simple picture are shown by the red dashed lines (6 for $d_{5/2}$ and 1 for $s_{1/2}$). For the neutrons, the occupancies for the sd orbitals ($d_{5/2}$ not shown) in the simple picture are shown by red dotted lines and for the $f_{7/2}$ orbital (1,3,5 for ^{36,38,40}P, respectively) by the green dashed-dotted line.

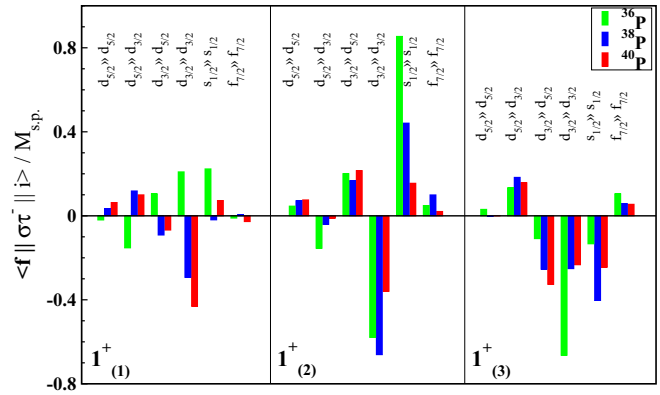

FIG. 6. Gamow-Teller matrix elements (M_{fi}) for the 1^+ states in ^{36,38,40}P decomposed into orbital components. The matrix elements have been normalized to the single-particle estimates ignoring the phase ($s_{1/2} \to s_{1/2} = 1.414$; $d_{5/2} \to d_{5/2} = 1.67$; $d_{5/2} \to d_{3/2} = 1.79$; $d_{3/2} \to d_{5/2} = 1.79$; $d_{3/2} \to d_{3/2} = 0.89$; $f_{7/2} \to f_{7/2} = 1.85$).

to the quenching of the $N = 28$ shell gap. For the 1p1h 1^+ states, the neutron excitation originates mainly from the $\nu d_{3/2}$ orbital with some contribution from $\nu s_{1/2}$ which increases for the higher 1^+ states.

Looking at the proton and neutron occupancies clearly suggests that for ^{40}P, the ground state as well as the low-lying observed excited states have quite complex configurations. In the macroscopic picture, this implies that ^{40}P has a deformed structure, corroborating results which suggest that nuclei with $Z \approx 14$ and $N \approx 28$ are deformed [30,31]. Deformation can result in mixing of states, and hence the increased complexity of the wave functions of the ground state as well as the excited states. The level spacing between the 1^+ states also decreases going from ^{36}P to ^{40}P consistent with strong mixing. We can expect these states to be even closer or degenerate for ^{42}P as we approach $N = 28$.

It is also to be noted from Fig. 3 that the first 1^+ state in both ^{38,40}P have the smallest absolute branching in the corresponding β decay. Though the lowest energy state of a given spin and parity should be favored by the large β-decay energy available, the transition to a particular state in the daughter nucleus is also dependent on the change in nuclear structure, or the wave-function overlaps. The GT matrix elements ($M_{\rm fi}$) from the shell model calculations, which measure the overlap between the initial and final state, are displayed in Fig. 6 for ^{36,38,40}P. The matrix elements have been decomposed into the orbital components and normalized to the single-particle estimates [32]. As can be seen from Fig. 6, the $M_{\rm fi}$ components for the 1^+_1 state are the smallest for both ^{38,40}P, with phases canceling each other leading to a large $\log ft$ value. Generally, a rearrangement of many nucleons could severely inhibit the decay, in some cases by an order of magnitude. From Fig. 5, the lowest 1^+ states have the simplest structure, predominantly $(\pi s^1_{1/2} \otimes \nu d^{-1}_{3/2})$ for the sd orbitals and are not connected to the Si ground state $(\pi d^6_{5/2} \otimes \nu d^4_{3/2})$ by an allowed one-body transition. For the same reason the β decay to the 1^+ ground state of ^{34}P is weaker than to the excited 1^+ state (see Fig. 4).

The $1^+_{2,3}$ states, on the other hand, have dominant components $(\pi d^1_{3/2} \otimes \nu d^{-1}_{3/2})$ and $(\pi s^1_{1/2} \otimes \nu s^{-1}_{1/2})$ which are connected by allowed transitions to the parent ground state. As shown in Fig. 6, the allowed $\nu d_{3/2} \to \pi d_{3/2}$ and $\nu s_{1/2} \to \pi s_{1/2}$ transitions are the strongest for these excited states, leading to the small observed $\log ft$ values. These strong matrix elements highlight the active vacancies, namely, $s_{1/2}$ and $d_{3/2}$. They also highlight that in neutron-rich nuclei, with neutrons and protons occupying different shells the GT decay of valence neutrons (in $f_{7/2}$) is retarded and it is the decay of the core neutrons that dominates. The smaller $\log ft$ values to the states with more complex structure involving excitation of protons and neutrons implies larger overlap with the ground state of the parent nucleus. This in turn emphasizes the deformed and hence complex nature of the parent ^{38,40}Si ground states too.

IV. SUMMARY AND CONCLUSIONS

The β decays of neutron-rich ^{38,40}Si were investigated at the NSCL, populating low-lying 1p1h states in the odd-odd daughter nuclei ^{38,40}P. Based on the allowed nature of the measured $\log ft$ values, these states have been assigned a J^π of 1^+. β-decay properties for the parent isotopes were also determined accurately. The half-life of ^{38}Si was measured to be 63(8) ms for the first time, while for ^{40}Si the half-life was extracted following the γ rays in ^{40}P leading to a value of 27.6(14) ms, a value smaller than the literature number. The β-delayed neutron emission probability was also extracted for ^{38}P and ^{40}P. Both the measured half-lives and P_n values agree quite well with the shell model calculations presented in this paper.

The observed 1p1h states in ^{38,40}P lie at a relatively low excitation energy in spite of the $N = 20$ shell gap. This

highlights the gain in pairing and correlation energy with neutrons occupying the $f_{7/2}$ orbital. Shell model calculations with the SDPF-MU interaction give a good description of these core-excited states in ^{38,40}P. However, the agreement is not as good for ^{36}P, suggesting that further refinement of the interaction is possible.

Examination of the shell model occupancies for both protons and neutrons reveals quite a complex configuration of the 1^+ states. The complexity of the states increases with neutron number and excitation energy. This can be understood in terms of the deformation-driving tendency of the $f_{7/2}$ neutron leading to mixed states. The narrowing of the level spacing between the 1^+ states with increasing neutron number is a result of this mixing. The complex structure of the states, as well as the fragmented GT matrix elements for larger N alludes to the weakening of the $N = 28$ shell gap for the phosphorus isotopes approaching $N = 28$. Based on the calculated GT matrix elements, it can be seen that for neutron-rich nuclei, with valence proton and neutrons occupying opposite-parity shells, the allowed GT decay is dominated by the transformation of the core neutrons. It would be interesting to investigate the β^- decay of ^{42}Si in the future to understand the systematics better.

ACKNOWLEDGMENTS

The authors thank the NSCL operations staff for the excellent beam and support during the experiment. The work was supported by NSF Grants No. PHY-1401574 (FSU) and No. PHY-1102511 (NSCL), U.S. Department of Energy under Contracts No. DEAC02-05CH11231 (LBNL) and No. DE-SC0009883 (FSU), and the U.S. National Nuclear Security Agency under Awards No. DE-NA0000979 and No. DE-NA0002132. Authors also want to acknowledge support from JSPS KAKENHI (Japan), Grants No. 25870168 and No. 15K05094.

[1] M. Thoennessen and B. M. Sherrill, Nature **473**, 25 (2011).
[2] T. Otsuka, Phys. Scr. T **152**, 014007 (2013).
[3] A. Gade, Eur. Phys. J. A **51**, 118 (2015).
[4] W. Loveland, D. J. Morrissey, and G. T. Seaborg, *Modern Nuclear Chemistry* (Wiley, New York, 2006).
[5] M. Madurga, S. V. Paulauskas, R. Grzywacz, D. Miller, D. W. Bardayan, J. C. Batchelder, N. T. Brewer, J. A. Cizewski, A. Fijalkowska, C. J. Gross *et al.*, Phys. Rev. Lett. **117**, 092502 (2016).
[6] M. F. Alshudifat, R. Grzywacz, M. Madurga, C. J. Gross, K. P. Rykaczewski, J. C. Batchelder, C. Bingham, I. N. Borzov, N. T. Brewer, L. Cartegni *et al.*, Phys. Rev. C **93**, 044325 (2016).
[7] R. Chapman, A. Hodsdon, M. Bouhelal, F. Haas, X. Liang, F. Azaiez, Z. M. Wang, B. R. Behera, M. Burns, E. Caurier *et al.*, Phys. Rev. C **92**, 044308 (2015).
[8] S. Grevy, J. C. Angelique, P. Baumann, C. Borcea, A. Buta, G. Canchel, W. N. Catford, S. Courtin, J. M. Daugas, F. de Oliveira *et al.*, Phys. Lett. B **594**, 252 (2004).
[9] Y. Utsuno, T. Otsuka, B. A. Brown, M. Honma, T. Mizusaki, and N. Shimizu, Phys. Rev. C **86**, 051301 (2012).
[10] A. Gade and B. M. Sherrill, Phys. Scr. **91**, 053003 (2016)
[11] D. J. Morrissey *et al.*, Nucl. Instrum. Methods Phys. Res., Sect. B **204**, 90 (2003).
[12] N. Larson, S. Liddick, M. Bennett, A. Bowe, A. Chemey, C. Prokop, A. Simon, A. Spyrou, S. Suchyta, S. Quinn *et al.*, Nucl. Instrum. Methods Phys. Res., Sect. A **727**, 59 (2013).
[13] W. Mueller, J. Church, T. Glasmacher, D. Gutknecht, G. Hackman, P. Hansen, Z. Hu, K. Miller, and P. Quirin, Nucl. Instrum. Methods Phys. Res., Sect. A **466**, 492 (2001).
[14] C. Prokop, S. Liddick, B. Abromeit, A. Chemey, N. Larson, S. Suchyta, and J. Tompkins, Nucl. Instrum. Methods Phys. Res., Sect. A **741**, 163 (2014).
[15] V. Tripathi, S. L. Tabor, C. R. Hoffman, M. Wiedeking, A. Volya, P. F. Mantica, A. D. Davies, S. N. Liddick, W. F. Mueller, A. Stolz, B. E. Tomlin, T. Otsuka, and Y. Utsuno, Phys. Rev. C **73**, 054303 (2006).
[16] N. Nica, J. Cameron, and B. Singh, Nucl. Data Sheets **113**, 1 (2012).
[17] M. Wang, G. Audi, A. H. Wapstra, F. G. Kondev, M. MacCormick, X. Xu, and B. Pfeiffer, Chin. Phys. C **36**, 1603 (2012).
[18] ENSDF database, http://www.nndc.bnl.gov/ensdf/
[19] O. Sorlin, Zs. Dombradi, D. Sohler, F. Azaiez, J. Timar, Yu.-E. Penionzhkevich, F. Amorini, D. Baiborodin, A. Bauchet, F. Becker *et al.*, Eur. Phys. J. A **22**, 173 (2004).
[20] A. Hodsdon, R. Chapman, X. Liang, F. Haas, J. Ollier, E. Caurier, F. Nowacki, M.-D. Salsac, F. Azaiez, S. Beghini *et al.*, Phys. Rev. C **75**, 034313 (2007).
[21] http://www.nndc.bnl.gov/logft/
[22] J. P. Dufour, R. Del Moral, A. Fleury, F. Hubert, D. Jean, M. S. Pravikoff, H. Delagrange, H. Geissel, and K.-H. Schmidt, Z. Phys. A - At. Nucl. **324**, 487 (1986).
[23] A. Gade, B. A. Brown, D. Bazin, C. M. Campbell, J. A. Church, D. C. Dinca, J. Enders, T. Glasmacher, M. Horoi, Z. Hu *et al.*, Phys. Rev. C **74**, 034322 (2006).
[24] K. Steiger, S. Nishimura, Z. Li, R. Gernhuser, Y. Utsuno, R. Chen, T. Faestermann, C. Hinke, R. Krcken, M. Kurata-Nishimura *et al.*, Eur. Phys. J. A **51**, 117 (2015).
[25] A. M. Nathan and D. E. Alburger, Phys. Rev. C **15**, 1448 (1977).
[26] B. A. Brown and B. H. Wildenthal, Annu. Rev. Nucl. Part. Sci. **38**, 29 (1988).
[27] M. Honma, T. Otsuka, B. A. Brown, and T. Mizusaki, Eur. Phys. J. A **25**, 499 (2005).
[28] T. Otsuka, T. Suzuki, M. Honma, Y. Utsuno, N. Tsunoda, K. Tsukiyama, and M. Hjorth-Jensen, Phys. Rev. Lett. **104**, 012501 (2010).
[29] S. R. Stroberg, A. Gade, J. A. Tostevin, V. M. Bader, T. Baugher, D. Bazin, J. S. Berryman, B. A. Brown, C. M. Campbell, K. W. Kemper *et al.*, Phys. Rev. C **91**, 041302(R) (2015).
[30] I. Hamamoto, Phys. Rev. C **89**, 057301 (2014).
[31] S. Takeuchi, M. Matsushita, N. Aoi, P. Doornenbal, K. Li, T. Motobayashi, H. Scheit, D. Steppenbeck, H. Wang, H. Baba *et al.*, Phys. Rev. Lett. **109**, 182501 (2012).
[32] J. Suhonen, *From Nucleons to Nucleus: Concepts of Microscopic Nuclear Theory* (Springer, New York, 2007), p. 166.